JURNAL SAINS MATERI INDONESIA (JUSAMI)
ISSN: 1411-1098 (print), 2614-087X (online)
VOL. 27, ISSUE 1, 2026
DOI: https://doi.org/10.55981/jsmi.2026.12227

ORIGINAL ARTICLE

Enhanced Co_2 Adsorption Using Activated Carbon From Tea Stem Waste Via Activation–Carbonization Strategy

Edi Supriadi[1], Efriyana Kampai[2], Muhdarina[2], Joni Prasetyo[1], Yessie Widya Sari[3], Tanti Ardiyati[1], Ary Mauliva Hada Putri[1]

[1]Research Center for Chemistry, National Research and Innovation Agency, BJ.HABIBIE Science and Technology Area Serpong, South Tangerang, 15314, Indonesia
[2]Department of Chemistry, Faculty of Mathematics and Natural Sciences (FMIPA), Universitas Riau, Pekanbaru, Indonesia
[3]Department of Physics, Institut Pertanian Bogor, Bogor, West Java, Indonesia

ABSTRACT – Tea stem agroindustrial waste, rich in cellulose, hemicellulose, and lignin, presents a promising low-cost precursor for sustainable activated carbon production. This study explores the activation–carbonization approach for synthesizing porous activated carbon and evaluates its effectiveness for CO_2 capture. Chemical activation was conducted using 60% w/v KOH at different activator-to-precursor ratios (0.5:1, 1:1, and 2:1 v/w), followed by carbonization at 250°C, 350°C, and 450°C in a fixed-bed pyrolysis reactor under nitrogen atmosphere. Among all samples, A1-450 0.5 (450°C, 0.5:1 ratio) exhibited the highest CO2 adsorption capacity (1.9500 mmol g^{-1}), attributed to its high surface area (679.4 m^2 g^{-1}) and predominantly microporous structure. XRD analysis confirmed the presence of disordered graphitic domains with broad peaks at 2θ = 22° and 44°, while FTIR revealed abundant surface functional groups (OH, C=C, CO) essential for CO2 interactions. SEM-EDX characterization showed a heterogeneous porous surface and high carbon content (78.23%). These findings demonstrate that the activation–carbonization route is more effective than carbonization–activation in producing high-performance bio-based CO_2 adsorbents, offering a viable strategy for valorizing agro-waste into functional carbon materials.

ARTICLE HISTORY
Received: 3 Juli 2025
Revised: 20 Aug 2025
Accepted: 1 Sep 2025

KEYWORDS
Activated carbon
Tea stem waste
Activation-carbonization
CO2 adsorption
Surface Characterization

INTRODUCTION

The accelerating threat of climate change, largely driven by the excessive release of greenhouse gases (GHGs) such as carbon dioxide (CO_2), has intensified global efforts to develop efficient carbon capture and storage (CCS) technologies. Among the various CCS methods, adsorption using porous solid sorbents has gained significant attention due to its energy efficiency, reversibility, and tunability [1]. In particular, activated carbon derived from renewable biomass has emerged as a promising class of adsorbents owing to its low cost, environmental friendliness, and high surface reactivity [1-3].

Agricultural residues represent an abundant and underutilized resource for activated carbon production. Many of these wastes—especially those rich in lignocellulosic components (cellulose, hemicellulose, and lignin)—can be thermochemically converted into highly porous carbon materials [4]. Valorizing such residues not only contributes to waste reduction but also supports the circular bioeconomy. Numerous studies have explored the transformation of biomass sources like coconut shells, rice husks, palm kernel shells, and sawdust into high-performance activated carbon for gas purification and energy storage applications [5-8].

Tea (*Camellia sinensis*) is one of the most widely cultivated crops in tropical and subtropical regions, including Indonesia. According to the Central Bureau of Statistics (2022) [9], Indonesia produced approximately 137,800 tons of tea in 2021, with West Java accounting for 68% of national production. The tea industry generates significant quantities of agro-industrial waste, including tea stems and twigs, which are often discarded or underutilized [10]. Notably, tea stems contain up to 43.45% carbon, with cellulose (31.58%) as the dominant component, making them an attractive feedstock for porous carbon synthesis [10].

Activated carbon is a highly porous material composed primarily of amorphous carbon. Its performance as an adsorbent depends critically on three key features: (i) specific surface area, (ii) pore structure (micro-, meso-, and macropores), and (iii)

***CORRESPONDING AUTHOR** | E. Supriadi | ✉ edisupriyadi127@gmail.com

surface chemistry, particularly the presence of functional groups such as hydroxyl, carbonyl, and carboxylic moieties [11]. These properties can be tailored through physical or chemical activation methods. Among them, chemical activation using potassium hydroxide (KOH) is widely favored for producing well-developed porosity and rich surface functionalities at moderate temperatures [11, 12].

The order of processing—whether activation precedes carbonization or vice versa—can significantly influence the resulting textural and chemical properties of activated carbon. In particular, activation–carbonization (AC) and carbonization–activation (CA) pathways may lead to different degrees of porosity, crystallinity, and surface

functionalization, which in turn affect the CO_2 adsorption performance [2, 13]. However, comparative studies on these synthesis routes using tea stem waste as precursor remain limited.

In this study, we present a comparative analysis of the activation–carbonization and carbonization–activation approaches for synthesizing activated carbon from tea stem agro-industrial waste. The impact of process parameters—such as activation ratio and carbonization temperature—on the physicochemical properties and CO_2 adsorption performance of the resulting materials is systematically investigated. A comprehensive suite of characterization techniques, including Brunauer–Emmett–Teller (BET) surface area analysis, Fourier Transform Infrared Spectroscopy (FTIR), X-ray Diffraction (XRD), and Scanning Electron Microscopy coupled with Energy Dispersive X-ray (SEM-EDX), is employed to elucidate the structural and chemical transformations during synthesis. The outcomes of this work contribute to the optimization of biomass valorization strategies for efficient carbon capture applications.

EXPERIMENTAL METHOD

Materials

In this study, tea stems (Camellia sinensis) were collected from tea plantations in Bogor, West Java, Indonesia. This region was selected because West Java accounts for the majority of Indonesia's tea production, providing a large and consistent supply of agro-waste with stable composition. The uniform cultivation practices and high production volume ensure reproducibility of precursor quality, which is crucial for reliable activated carbon synthesis.

Prior to use, the stems were washed with distilled water, sun-dried, and then oven-dried at 60°C for 48 hours, following procedures reported in previous studies on biomass pretreatment [10, 14, 15]. The dried stems were ground into a fine powder and sieved through 170 and 200 mesh screens (~75–90 μm) to obtain uniform particle sizes. The use of this size range was based on its balance between surface accessibility and processability. Particles finer than 200 mesh (<75 μm) often exhibit excessive agglomeration and poor flowability, which can reduce the efficiency of impregnation and complicate subsequent washing and filtration steps. Conversely, particles coarser than 170 mesh (>90 μm) provide less external surface area and limit contact between the biomass precursor and the KOH solution, thereby hindering uniform pore development during activation. Thus, the 170–200 mesh fraction was chosen to maximize surface–activator interactions while maintaining good handling and reproducibility in the activation–carbonization process [5, 16].

Reagents and chemicals used in this study included potassium hydroxide (KOH, EMSURE®, Supelco), hydrochloric acid (HCl, technical grade), acetone (C_3H_6O, technical grade), and distilled water (H_2O). High-purity nitrogen gas (N_2, research grade) was used as the inert carrier gas during the carbonization process.

Synthesis of Activated Carbon

Chemical Activation

Chemical activation was conducted by mixing 5 g of sieved tea stem powder with 60% (w/v) KOH solution at varying activator-to-precursor ratios of 0.5:1, 1:1, and 2:1 (v/w). The mixture was stirred at 110 rpm for 3 hours at 80°C using a Bante magnetic stirrer (Model MS300, Bante Instruments, China). After activation, the samples were filtered and thoroughly washed with 1 N HCl solution, followed by distilled water until a neutral pH (pH = 7) was reached. The resulting solids were dried in a Memmert UN110 oven (Memmert GmbH, Germany) at 110°C for 24 hours.

Carbonization

Carbonization was carried out in a fixed-bed pyrolysis reactor (custom-built stainless steel, equipped with a PID temperature controller and continuous N_2 flow system; Figure 1) under a constant flow of nitrogen gas (5 mL/min) to maintain an inert atmosphere. The activated samples were subjected to pyrolysis at three target temperatures: 250°C, 350°C, and 450°C. The heating rate was set at 5°C/min, and the residence time at the final temperature was maintained for 5 hours. Samples were labeled according to the synthesis route, carbonization temperature, and impregnation ratio, as summarized in Table 1.

Characterization Techniques

Morphological and Elemental Analysis (SEM–EDX)

The surface morphology and elemental composition of the activated carbon samples were analyzed using a Scanning Electron Microscope coupled with Energy Dispersive X-ray Spectroscopy (SEM–EDX, Hitachi SU3500). The images were obtained at a magnification of 3000× to evaluate pore structure and surface features.

Table 1. Sample Codes and Synthesis Conditions for Tea Stem-Based Activated Carbon

Method	Temperature (°C)	Activator-to-Precursor Ratio (v/w)	Sample Code
Activation-Carbonization	250	0.5:1	A1-250 0.5
		1:1	A1-250 1
		2	A1-250 2
	350	0.5:1	A1-350 0.5
		1:1	A1-350 1
		2	A1-350 2
	450	0.5:1	A1-450 0.5
		1:1	A1-450 1
		2	A1-450 2

Functional Group Analysis (FTIR)

Fourier Transform Infrared (FTIR) spectroscopy was employed to identify the surface functional groups present on the activated carbon samples. The analysis was performed using a Thermo Scientific Nicolet iS10 spectrometer (Thermo Fisher Scientific, USA) in the wavenumber range of 4000–500 cm^{-1}.

Crystallographic Structure (XRD)

The crystalline structure and average crystallite size were determined by X-ray Diffraction (XRD) using a Rigaku SmartLab diffractometer (Rigaku, Japan) equipped with a Cu-Kα anode (λ = 1.5406 Å), operated at 40 kV and 30 mA. Diffraction patterns were recorded in the 2θ range of 10°–60° with a step size of 0.02° and a scan speed of 2°/min.

Textural Properties (BET)

The specific surface area, total pore volume, and average pore diameter were obtained from nitrogen adsorption–desorption isotherms at 77 K using a Micromeritics ASAP 2020 instrument (Micromeritics, USA).

Proximate Analysis

Proximate analysis of the activated carbon samples, including moisture content, ash content, volatile matter, and fixed carbon, was conducted according to ASTM D5832-98 standard procedures.

CO_2 Adsorption Performance

The CO_2 adsorption capacity was measured using a Micromeritics AutoChem II 2920 instrument equipped with a TPD-CO_2 module. A 0.05 g sample was pre-treated at 150°C for 30 minutes under helium flow to remove surface moisture. Adsorption was carried out at 25°C using a 5% CO_2/He gas mixture (v/v) for 90 minutes. Desorption was then performed under helium purge, ramping the temperature from 25°C to 200°C at a rate of 10°C/min.

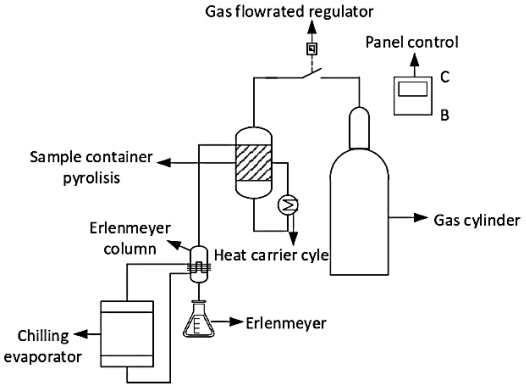

Figure 1. Schematic Diagram of The Fixed-Bed Pyrolysis Reactor Used for Carbonization.

RESULT AND DISCUSSION

Yield of Activated Carbon

The yield of activated carbon derived from tea stem waste decreased with increasing carbonization temperature and KOH impregnation ratio (Figure 2). This trend is attributed to the enhanced devolatilization and thermal degradation of lignocellulosic components at elevated temperatures, which results in greater mass loss during pyrolysis [16]. Similarly, a higher KOH-to-precursor ratio promotes the formation of micropores through chemical etching, consuming more carbon atoms and reducing the final yield [5]. The lowest yield was observed for samples synthesized at 450°C with a 2:1 ratio, indicating a trade-off between pore development and carbon recovery.

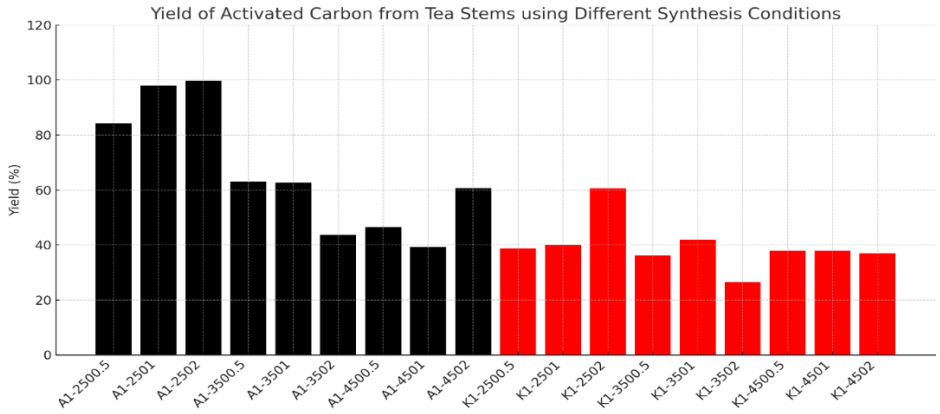

Figure 2. Comparison of Activated Carbon Yield Obtained from Tea Stem Waste Using Activation–Carbonization and Carbonization–Activation Methods

Proximate Analysis

Proximate analysis results (Table 2) show that all activated carbon samples meet the Indonesian National Standard (SNI 06-3730-1995) for water content (<15%), ash content (<10%), and volatile matter (<15%). The water content was lowest in A1-450 2 (4.84%), highlighting the effectiveness of high-temperature carbonization in removing moisture. A1-250 1 exhibited the highest fixed carbon content (89.08%), likely due to optimal retention of carbonaceous matter at moderate activation ratios. Ash content was generally low, indicating minimal mineral residue that could obstruct the pore structure. The fixed carbon content increased with decreasing volatile matter, suggesting more complete carbonization and enhanced adsorbent stability [11].

Table 2. Comparison of Proximate Composition (Moisture, Ash, Volatile Matter, and Fixed Carbon) of Activated Carbon Synthesized Using Different Methods

Activated carbon	Water content (%)	Ash Content (%)	Volatile Matter Level (%)	Bound Carbon (%)
K1-250-0.5	12.00	7.59	3.80	76.61
K1-250-1	11.34	8.08	5.29	75.29
K1-250-2	8.52	0.60	5.49	85.39
K1-350-0.5	11.11	2.69	6.89	79.31
K1-350-1	11.2	2.20	12.67	73.61
K1-350-2	11.89	1.30	18.86	67.95
K1-450-0.5	12.88	2.00	13.55	71.56
K1-450-1	11.28	9.57	8.48	70.67
K1-450-2	11.66	5.38	13.55	69.41
A1-250-0.5	13.97	7.78	11.76	66.49
A1-250-1	5.63	1.20	4.09	89.08
A1-250-2	10.21	4.79	12.65	72.35
A1-350-0.5	13.86	6.09	15.77	64.28
A1-350-1	5.80	0.90	19.98	73.32
A1-350-2	6.07	2.80	13.83	77.30
A1-450-0.5	6.81	2.40	16.95	73.84
A1-450-1	10.02	7.29	12.99	69.70
A1-450-2	4.84	1.00	11.16	83.00
SNI	≤15	≤10	≤15	≤60

Surface Area and CO_2 Adsorption Capacity

The specific surface area and pore structure significantly influence the adsorption performance of activated carbon. BET analysis revealed that sample A1-450 0.5 achieved the highest surface area (679.4 $m^2 g^{-1}$), while K1-250 0.5 exhibited the lowest (86.6 $m^2 g^{-1}$). The CO_2 adsorption capacities followed the same trend, with A1-450 0.5 attaining 1.9500 mmol g^{-1} and K1-250 0.5 reaching only 0.6451 mmol g^{-1} (Figure 4). The superior adsorption performance of A1-450 0.5 is attributed to the well-developed microporosity and accessible adsorption sites generated by the activation-carbonization route. Microporous carbon structures have been shown to enhance CO_2 uptake through size exclusion and van der Waals interactions [13].

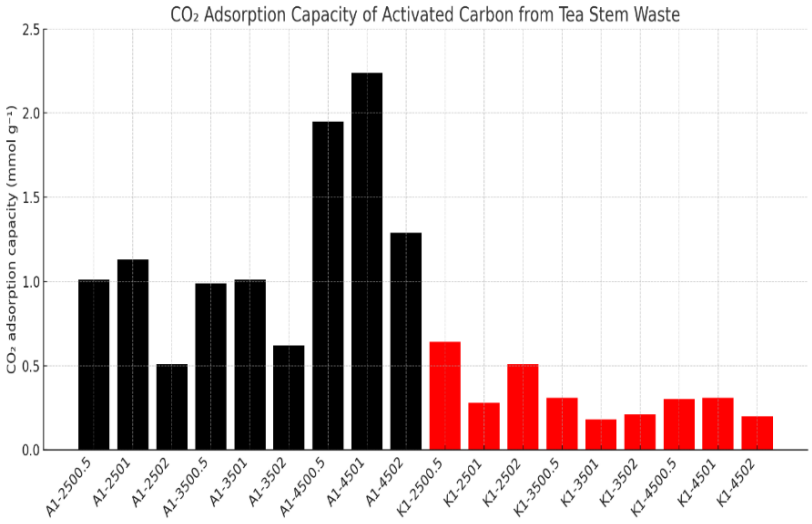

Figure 3. CO2 Adsorption Capacity (mmol g^{-1}) Of Activated Carbon Synthesized from Tea Stem Waste using Activation–Carbonization (A1-Series, Black) And Carbonization–Activation (K1-Series, Red) Methods under Various Synthesis Conditions

Surface Functional Groups (FTIR Analysis)

The FTIR spectra of the raw tea stem material, A1-450 0.5, and K1-250 0.5 (Figure 4) reveal the presence and transformation of various oxygen-containing functional groups due to different synthesis methods. These changes are critical for understanding the adsorption behavior of CO_2 on the activated carbon surface.

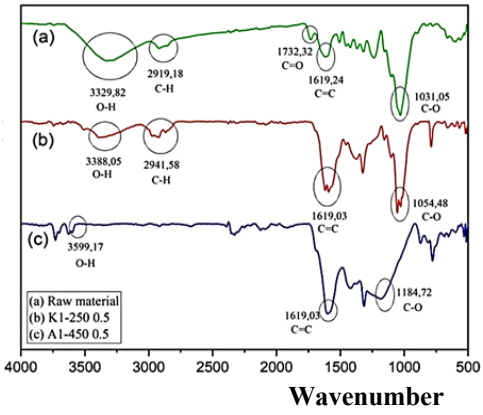

Figure 4. FTIR Spectra of Raw Tea Stem, A1-450 0.5, and K1-250 0.5, Showing the Transformation of Functional Groups as Influenced by Different Synthesis Methods

Broad absorption bands observed around 3300–3600 cm^{-1} in all spectra are attributed to O–H stretching vibrations, indicative of hydroxyl and phenolic groups [14, 17]. These peaks are prominent in the raw material and K1-250 0.5, but significantly reduced in A1-450 0.5. This reduction suggests the dehydration and thermal degradation of hydroxyl groups during high-temperature treatment (450°C), leading to a more carbonized and hydrophobic surface.

In the raw material, a distinct CH stretching peak is observed at 2919 cm^{-1}, corresponding to aliphatic C–H bonds from cellulose and hemicellulose. This peak persists in K1-250 0.5 (2941 cm^{-1}) but disappears completely in A1-450 0.5,

confirming the thermal decomposition of aliphatic hydrocarbons under more severe carbonization conditions [11]. This absence of aliphatic CH groups in A1-450 0.5 indicates a higher degree of carbonization, contributing to a more graphitic and porous carbon matrix, which enhances CO_2 adsorption [10].

Peaks in the range of 1700–1750 cm^{-1} are assigned to C=O stretching vibrations, representing carbonyl or carboxylic acid groups. The presence of C=C stretching peaks near 1600 cm^{-1} suggests aromatic structures, while bands at 1000–1300 cm^{-1} correspond to C–O stretching of ether, ester, or phenolic groups. These oxygenated groups are known to act as active sites for CO_2 adsorption, facilitating interaction via dipole–quadrupole forces and π–π interactions [12][18].

The observed spectral differences between A1-450 0.5 and K1-250 0.5 indicate that activation–carbonization (A1) results in a lower concentration of polar functional groups but a higher carbon structure regularity, favoring physisorption and π–π electron donor–acceptor interactions [18]. Conversely, the carbonization–activation (K1) method retains more polar groups, potentially enhancing chemical interaction with CO_2, though this may be offset by lower porosity or surface area.

Overall, the FTIR analysis confirms that both the chemical composition and structural evolution of surface functional groups are strongly affected by synthesis route and temperature. These differences play a crucial role in defining the adsorption performance of tea stem-based activated carbon toward CO_2. The spectral changes—including peak shifts, intensity reductions, and new band formations—reflect the breakdown of complex lignocellulosic structures into simpler functional moieties during pyrolysis and activation processes [19, 20].

Structural Crystallinity (XRD Analysis)

The crystallinity and structural order of the activated carbon samples were examined using X-ray diffraction (XRD), as presented in Figure 5. Although the CO_2 adsorption capacity of A1-450 1 was slightly higher, the A1-450 0.5 sample was chosen for XRD characterization because it represents a more optimal balance between surface area, yield, and crystallinity, and showed more consistent results across repeated experiments.

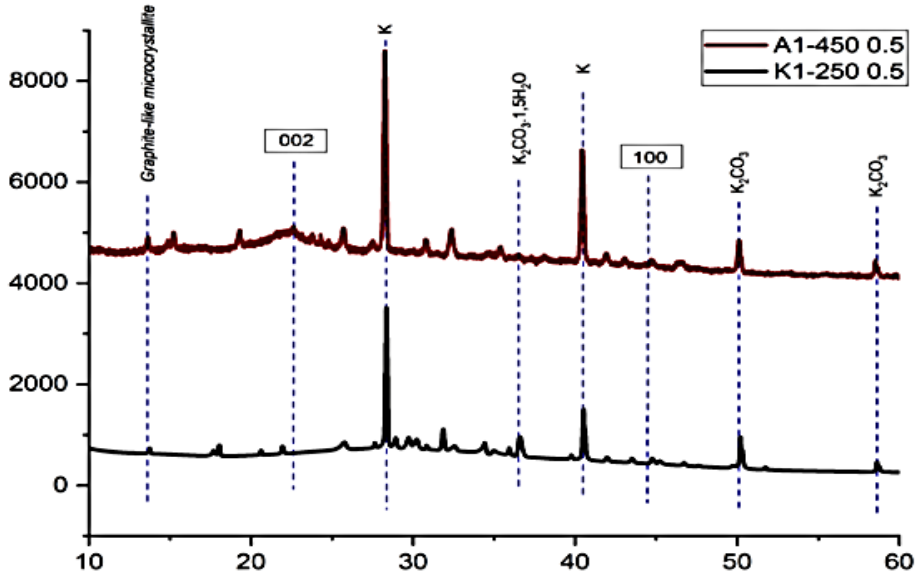

Figure 5. XRD Diffractograms of Activated Carbon A1-450 0.5 and K1-250 0.5, Indicating Differences in Crystallinity and Structural Order

Both samples, A1-450 0.5 and K1-250 0.5, exhibit two broad diffraction peaks located at approximately 2θ = 22° and 2θ = 44°, corresponding to the (002) and (100) planes of turbostratic graphite, respectively. These peaks are characteristic of disordered or partially graphitic carbon, which is typical of activated carbon materials derived from lignocellulosic biomass. The assignments are consistent with the reference pattern JCPDS No. 86-1157.

The (002) reflection near 22° indicates the stacking of aromatic layers, while the (100) peak around 44° reflects in-plane structural order [15, 21] . The broader and more diffuse peak in A1-450 0.5 implies a greater degree of disorder but still retains partial graphitic features, suggesting moderate crystallinity. In contrast, K1-250 0.5 exhibits slightly sharper and narrower peaks, which may reflect a more amorphous structure, indicating limited development of graphitic domains at the lower activation temperature.

Table 3. Crystallinity, amorphous content, and average crystallite size of activated carbon samples

Activated Carbon	Crystal Area	Total Area	Amorphous (%)	Crystal (%)	Average Crystal Size (nm)
A1-450-0.5	16922.87	22497.34	24.77	75.22	22.0658
K1-250-0.5	26277.83	29760.46	11.70	88.29	31.8998

Quantitative analysis of crystallinity (Table 3) shows that A1-450 0.5 exhibits a higher crystalline fraction (75.22%) compared to K1-250 0.5 (63.50%), despite the broader peak appearance. This result suggests that the activation–carbonization route (A1) at elevated temperatures promotes more effective structural ordering than the carbonization–activation route (K1), which is constrained by lower thermal energy. Additionally, A1-450 0.5 has a smaller average crystallite size (22.07 nm) compared to K1-250 0.5 (31.90 nm), indicating finer and more numerous crystalline domains that contribute to higher surface reactivity and pore development.

A clear correlation was observed between the crystallite size, degree of crystallinity, and CO_2 adsorption capacity. The A1-450 0.5 sample, which exhibited a smaller crystallite size (22.07 nm) and a higher crystalline fraction (75.22%), demonstrated significantly higher CO_2 uptake (1.95 mmol g^{-1}) compared to K1-250 0.5 (31.90 nm, 63.50%, 0.65 mmol g^{-1}). Smaller crystallite size generally provides more active edge sites and defect structures, enhancing CO_2 adsorption through van der Waals interactions and electrostatic attraction. In addition, the higher crystalline fraction improves structural stability and favors micropore development, thereby increasing the accessible surface area for adsorption. These findings suggest that both crystallite refinement and improved ordering contribute positively to CO_2 capture performance, in agreement with previous reports [17,19].

The XRD patterns also show minor background signals, likely arising from residual potassium compounds such as K_2CO_3 and $KOH{\cdot}H_2O$, especially in K1-250 0.5. These species may result from incomplete removal of activating agents or the interaction of KOH with atmospheric moisture and CO_2, as KOH is highly hygroscopic [22]. Although the KOH impregnation at 80 °C is relatively mild, it may initiate secondary reactions that leave crystalline by-products detectable by XRD.

From a functional perspective, the enhanced crystallinity and reduced crystallite size in A1-450 0.5 are advantageous, as they correlate with better electrical conductivity, surface reactivity, and structural stability, all of which are beneficial for CO_2 adsorption and potential regeneration cycles [3, 23].

Surface Morphology and Elemental Composition (SEM–EDX)

The surface morphology and elemental composition of the activated carbon samples were examined using Scanning Electron Microscopy (SEM) and Energy Dispersive X-ray Spectroscopy (EDX), as shown in Figure 6 and Table 4. These characterizations provide insights into the pore structure and elemental constituents, which are critical for understanding the material's adsorption performance.

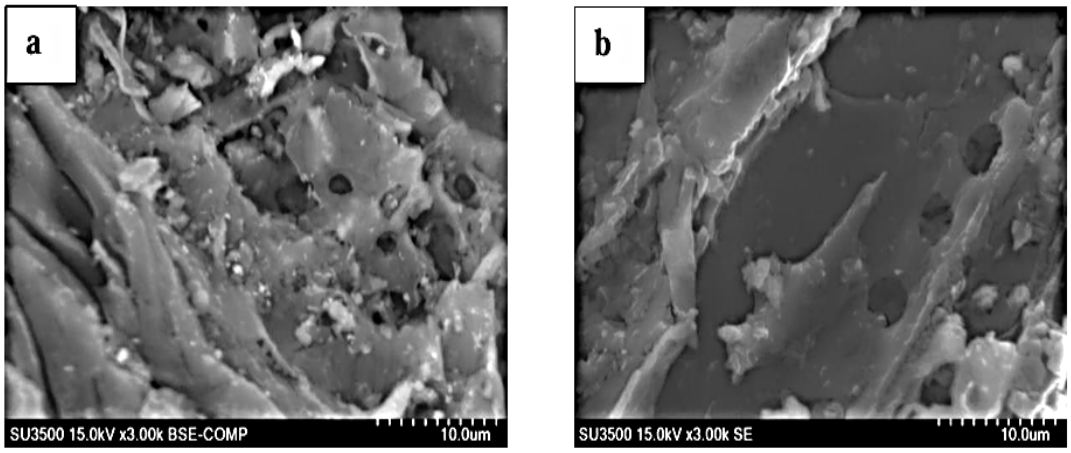

Figure 6. SEM Images of (a) A1-450 0.5 and (b) K1-250 0.5 at 3000× Magnification Showing Differences in Porosity and Surface Roughness.

Surface Morphology (SEM Analysis)

SEM micrographs at 3000× magnification (Figure 6) reveal notable differences in the surface textures of the two samples. A1-450 0.5, prepared via the activation–carbonization route at 450 °C, exhibits a highly heterogeneous and porous structure, with the appearance of well-developed cavities and disordered pore networks. These morphological features suggest that the higher pyrolysis temperature enhances volatile release and promotes pore development [6, 7].

In contrast, K1-250 0.5, synthesized using the carbonization–activation method at a lower temperature (250 °C), shows a smoother and more compact surface with limited visible porosity. The insufficient thermal energy likely inhibits the full decomposition of organic matter and hinders the expansion of internal pore walls, resulting in a lower overall surface area and fewer adsorption-active sites.

Elemental Composition (EDX Analysis)

Table 4. Elemental Composition (%Wt) of Activated Carbon Samples Based on EDX Analysis.

Element	A1-450-0.5	K1-250-0.5
	Heavy (%)	
C	78.23	63.50
O	10.11	25.19
Mg	0.24	0.21
CI	0.59	0.85
K	9.93	10.25
Ca	0.90	-
Total (%)	100.00	100.00

EDX analysis (Table 4) was employed to determine the elemental distribution in both activated carbon samples. The results indicate that carbon (C) is the dominant element, with a significantly higher content in A1-450 0.5 (78.23%) compared to K1-250 0.5 (63.50%). This higher carbon content in A1-450 0.5 is attributed to the more complete thermal decomposition of non-carbon elements, such as oxygenated volatiles and functional groups, during high-temperature carbonization. In contrast, the elevated oxygen (O) content in K1-250 0.5 (25.19%) reflects the less efficient carbonization process under milder thermal conditions.

Potassium (K) was detected in both samples: 9.93% for A1-450 0.5 and 10.25% for K1-250 0.5. The presence of K is likely due to residual KOH from the chemical activation step. Inadequate washing with HCl may have resulted in incomplete removal of potassium-containing compounds, which can remain embedded within the carbon matrix [8]. This residual K may also affect the surface basicity and thermal stability of the activated carbon [24].

Minor elements such as magnesium (Mg), chlorine (Cl), and calcium (Ca) were also identified. These are presumed to originate from the inorganic content of the raw tea stem biomass, as lignocellulosic materials naturally contain small amounts of mineral matter. While these elements are present in low concentrations, they may subtly influence the surface chemistry or regeneration behavior of the adsorbent [24, 25]. However, their overall contribution to CO_2 adsorption performance is considered negligible under the conditions tested.

CONCLUSION

Activated carbon synthesized from tea stem agro-industrial waste using the activation–carbonization method exhibits physicochemical properties that meet the Indonesian National Standard (SNI 06-3730-1995) for proximate parameters, including moisture, ash, volatile matter, and fixed carbon content. This synthesis route proved to be more effective for CO_2 adsorption than the conventional carbonization–activation sequence.

Among all samples, A1-450 0.5, produced at 450°C with a 0.5:1 activator-to-precursor ratio, demonstrated the highest CO_2 adsorption capacity (1.9500 mmol g^{-1}). This superior performance is attributed to its well-developed textural and structural properties, including a high specific surface area (679.4 m^2 g^{-1}) and a larger average pore diameter (10.76 nm), compared to sample K1-250 0.5 (86.6 m^2 g^{-1}; 2.61 nm). XRD analysis revealed that A1-450 0.5 possesses a partially graphitic structure with broad diffraction peaks at 2θ = 22° and 44°, and a smaller crystallite size (22.06 nm), indicating enhanced carbon ordering. Morphologically, both samples exhibited heterogeneous and irregular pore structures, as confirmed by SEM analysis. Chemically, A1-450 0.5 contained a higher carbon content (78.23%) and lower oxygen content (10.11%) than K1-250 0.5 (63.50% C, 25.19% O), indicating more effective devolatilization and carbonization at elevated temperatures. FTIR analysis showed the presence of OH, C=C, and C–O functional groups in both samples, while the absence of CH stretching in A1-450 0.5 further confirms the decomposition of aliphatic structures during high-temperature treatment. Overall, this study demonstrates that the activation–carbonization approach offers a promising strategy for converting tea stem waste into high-performance activated carbon suitable for CO_2 capture applications.

REFERENCES

[1] M. Hanifa *et al.*, "A review on CO2 capture and sequestration in the construction industry: Emerging approaches and commercialised technologies," *Journal of CO2 Utilization*, vol. 67, p. 102292, 2023.

[2] J. Serafin and B. Dziejarski, "Activated carbons—preparation, characterization and their application in CO2 capture: A review," *Environmental Science and Pollution Research*, 2023.

[3] Z. Heidarinejad *et al.*, "Methods for preparation and activation of activated carbon: a review," *Environmental Chemistry Letters*, vol. 18, pp. 393-415, 2020.

[4] V. K. Singh and E. A. Kumar, "Comparative Studies on CO2 Adsorption Kinetics by Solid Adsorbents," *Energy Procedia*, vol. 90, pp. 316-325, 2016.

[5] M. Sevilla and A. B. Fuertes, "Sustainable porous carbons with a superior performance for CO2 capture," *Energy & Environmental Science*, vol. 4, no. 5, pp. 1765-1771, 2011.

[6] J. Pallarés, A. González-Cencerrado, and I. Arauzo, "Production and characterization of activated carbon from barley straw by physical activation with carbon dioxide and steam," *Biomass and Bioenergy*, vol. 115, pp. 64-73, 2018.

[7] D. Li *et al.*, "Preparation of porous carbons with high low-pressure CO2 uptake by KOH activation of rice husk char," *Fuel*, vol. 139, pp. 68-70, 2015.

[8] E. N. Nunes *et al.*, "Characterization of yellow mombin biomass (Spondias mombin L.) for production of activated carbon," *Journal of Thermal Analysis and Calorimetry*, vol. 135, no. 6, pp. 3281-3288, 2019.

[9] B. P. Statistik, *Indonesia Tea Statistics 2023*, Jakarta: Badan Pusat Statistik, 2023.

[10] A. M. H. Putri *et al.*, "Performance of activated carbon derived from tea twigs for carbon dioxide adsorption," *Current Research in Green and Sustainable Chemistry*, vol. 10, p. 100440, 2025.

[11] S. F. Saifuddin *et al.*, "Characteristics of activated carbon derived from seaweed solid waste using chemical activation," *AIP Conference Proceedings*, vol. 2902, no. 1, 2023.

[12] K. Aprilio *et al.*, "Synthesis and characterization of MOFs/activated carbon composite on carbon-dioxide adsorption," *AIP Conference Proceedings*, vol. 2902, no. 1, 2023.

[13] A. K. H. P. S. *et al.*, "Activated Carbon from Various Agricultural Wastes by Chemical Activation with KOH: Preparation and Characterization," *Journal of Biobased Materials and Bioenergy*, vol. 7, pp. 1-7, 2013.

[14] J. Zhou, A. Luo, and Y. Zhao, "Preparation and characterisation of activated carbon from waste tea by physical activation using steam," *Journal of the Air & Waste Management Association*, vol. 68, no. 12, pp. 1269-1277, 2018.

[15] S. M. Yakout and G. Sharaf El-Deen, "Characterization of activated carbon prepared by phosphoric acid activation of olive stones," *Arabian Journal of Chemistry*, vol. 9, pp. S1155-S1162, 2016.

[16] C. A. Zaror and D. L. Pyle, "The pyrolysis of biomass: A general review," *Proceedings of the Indian Academy of Sciences Section C: Engineering Sciences*, vol. 5, no. 4, pp. 269-285, 1982.

[17] D. Dittmann *et al.*, "Characterization of activated carbons for water treatment using TGA-FTIR for analysis of oxygen-containing functional groups," *Applied Water Science*, vol. 12, no. 8, p. 203, 2022.

[18] T. Chen, M. Li, and J. Liu, "π–π Stacking Interaction: A Nondestructive and Facile Means in Material Engineering for Bioapplications," *Crystal Growth & Design*, vol. 18, no. 5, pp. 2765-2783, 2018.

[19] T. Pagketanang *et al.*, "Microporous Activated Carbon from KOH-Activation of Rubber Seed-Shells for Application in Capacitor Electrode," *Energy Procedia*, vol. 79, pp. 651-656, 2015.

[20] J. Wang *et al.*, "High-surface-area porous carbons produced by the mild KOH activation of a chitosan hydrochar and their CO2 capture," *New Carbon Materials*, vol. 36, no. 6, pp. 1081-1090, 2021.

[21] M. J. Lilian *et al.*, "Study of KOH-activated hydrochar for CO2 adsorption," *Journal of Industrial and Engineering Chemistry*, vol. 143, pp. 240-251, 2025.

[22] J. Y. Lai, L. H. Ngu, and S. S. Hashim, "A review of CO2 adsorbents performance for different carbon capture technology processes conditions," *Greenhouse Gases: Science and Technology*, vol. 11, no. 5, pp. 1076-1117, 2021.

[23] N. A. Zubbri *et al.*, "Low temperature CO2 capture on biomass-derived KOH-activated hydrochar established through hydrothermal carbonization with water-soaking pre-treatment," *Journal of Environmental Chemical Engineering*, vol. 9, no. 2, p. 105074, 2021.

[24] M. Gorbounov *et al.*, "Chemical activation of porous carbon extracted from biomass combustion bottom ash for CO2 adsorption," *Carbon Capture Science & Technology*, vol. 10, p. 100151, 2024.

[25] C. Goel *et al.*, "CO2 adsorption by KOH-activated hydrochar derived from banana peel waste," *Chemical Papers*, vol. 78, no. 6, pp. 3845-3856, 2024.